EPJ Web of Conferences **140**, 06015 (2017) DOI: 10.1051/epjconf/201714006015
Powders & Grains 2017

Comparison of multi-sphere and superquadric particle representation for modelling shearing and flow characteristics of granular assemblies

Behzad Soltanbeigi[1,⋆], *Alexander* Podlozhnyuk[2,⋆⋆], *Jin Y.* Ooi[1], *Christoph* Kloss[2,3], and *Stefanos-Aldo* Papanicolopulos[1]

[1] *Institute for Infrastructure and Environment, School of Engineering, The University of Edinburgh, EH9 3JL, Edinburgh, UK*
[2] *DCS Computing GmbH, Industriezeile 35, 4020, Linz, Austria*
[3] *CFDEMresearch GmbH, Industriezeile 35, 4020, Linz, Austria*

Abstract. In the current study, complex-shaped particles are simulated with the Discrete Element Method (DEM) using two different approaches, namely Multi-spheres (MS) and Superquadrics (SQ). Both methods have been used by researchers to represent the shape of real particles. However, despite the growing popularity of utilizing MS and SQ particles in DEM simulations, few insights have been given on the comparison of the macro scale characteristics arising from the two methods. In this respect, initially the characteristics of the two shape representation methods are evaluated in a direct shear test simulation. The results suggest that controlling the sharpness of the edges for SQ particles can lead to a good agreement with the results of MS particles. This way, a set of SQ and MS particles, which are numerically calibrated in the shear tester, are obtained. Furthermore, the macro-scale responses of the numerically calibrated particles are assessed during a slow shearing scenario, which is achieved through simulating quasi-static flow of the particles from a flat-bottom silo. The results for mass discharge, flow profile and wall pressure show a good quantitative agreement. These findings suggest that the numerically calibrated MS and SQ particles in the shear tester can provide similar bulk-scale flow properties. Moreover, the results highlight that surface bumpiness for MS particles and corner sharpness for SQ particles change the characteristics of particles and play a significant role in the shear strength of the material composed of these particles.

1 Introduction

Most DEM codes use spherical particles to reduce the computational cost of simulations, although in reality particles are mostly of irregular shape. Several non-spherical shape descriptions have been proposed in the literature, the most popular approach in DEM being the multi-sphere approach (MS) [1]. In this description, spheres are allowed to overlap and be glued together to approximate an arbitrarily shaped particle. Another shape description, recently implemented in the DEM package LIGGGHTS [2], is the superquadric (SQ) [3, 4] that is an extension of spheres and ellipsoids.

Several researchers have studied the characteristics of different shape representation methods and compared them at the micro and macro level. Cleary and Sawley [5] compared the discharge of SQ and spherical particles from a hopper and showed that the non-sphericity causes a slower flow up to 30% and also changes the flow kinematics. Fraige et al. [6] simulated spherical and cubical particles in a flat-bottom silo and concluded that cubic-shape particles provide a packing with lower porosity and increased resistance to flow compared to spheres. Tao et al. [7] used the MS approach to represent corn-shape particles and compared the flow properties with spherical particles. They showed that the downward velocity of the clusters shows higher variation, compared to spheres, along the width of the silo (from centre toward walls). Furthermore, they observed that the mean voidage of packings for non-spherical particles is smaller than that of the spherical particles. Markauskas et al. [8] evaluated the capability of MS to provide ellipsoidal particles, which can replace the perfectly smooth ellipsoids generated using the SQ technique. Assigning the variable parameter as the number of sub-spheres, the MS particles were characterized through studying the angle of repose, porosity and coordination numbers. It was pointed out that increasing the number of sub-spheres exhibits a clear tendency to mimic macroscopic parameters of a smooth ellipsoid.

Based on the above studies, it is clear that several attempts have been made to understand the characteristics of different shape approximation methods. However, there is still a lack of a comprehensive study that investigates the bulk response of the SQ and MS particles under various compression and shearing conditions. Accordingly, this paper aims to provide a better understanding of the micro/macro properties of the MS and SQ particles and also investigates the potential similarities. In this respect, a series of shearing tests, with MS and SQ particles in a

⋆e-mail: b.soltanbeigi@ed.ac.uk
⋆⋆e-mail: alexander.podlozhnyuk@dcs-computing.com

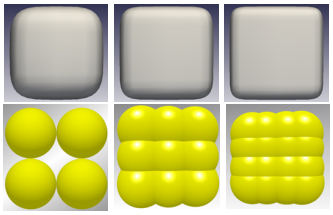

Figure 1. Particle shapes used. SQ_{N4},SQ_{N6} and SQ_{N8}, top, from left to right. And MS_8, MS_{27} and MS_{64}, bottom, from left to right

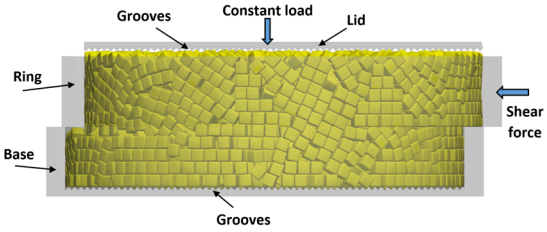

Figure 2. Jenike shear tester filled with superquadric particles

Jenike shear tester, are conducted to determine the role of edge sharpness in SQ and number of sub-spheres (surface bumpiness) in MS particles. Subsequently, the flow properties of SQ and MS particles with similar macroscopic shearing response, are evaluated through comparing various bulk-scale features during a silo discharge.

2 Methodology

This section provides information regarding material properties and testing procedures that have been followed. The considered particles have cubical shapes with edge length of $d = 2$mm. Cubes were approximated by SQ particles in LIGGGHTS and by MS particles in EDEM [9] (Fig.1). The considered material is selected from the Generic EDEM Material Model (GEMM) Database, which provides suitable material inputs for accurate representation of bulk materials. Table 1 shows the material properties for particles and geometry.

The equation that governs the shape of SQ particles, given by Barr [10], is as follows:

$$f(x,y,z) \equiv (|x/a|^{n_2} + |y/b|^{n_2})^{n_1/n_2} + |z/c|^{n_1} - 1 = 0.$$

A detailed description of a contact detection and a contact force algorithm for two SQ particles implemented in LIGGGHTS can be found in [4]. Cubical particles can be modelled by superquadrics taking $a = b = c = d/2$ and taking $n_1 = n_2 = N > 2$, where N controls the level of edge sharpness/blockiness. Different levels of edge sharpness ($N = 4, 6$ and 8, denoted as SQ_{N4}, SQ_{N6} and SQ_{N8} correspondingly, see Fig.1) were used in this paper.

Multispheres, which approximate the shape of particles by overlapping or touching of spheres, are used as an approximation of the real shape irregularities [1, 11]. Cubes were modelled in EDEM by multi-spheres using 8, 27 and 64 sub-spheres of equal radius (denoted as MS_8, MS_{27} and MS_{64} correspondingly, see Fig. 1).

The Jenike shear tester is widely used for measuring flow properties of particulate solids, [12]. In this test the granular material is placed in a split cylindrical box. Then, the material is consolidated by applying a constant vertical load σ_v to the lid section. Later, the top half of the cylinder (ring) is moved at a constant translational velocity (Fig.2). The measured quantity is the force required for this movement that can be converted to an average shear stress τ. The quasi-static flow of SQ and MS particles is further assessed in silo discharge. The flat-bottom silo has dimensions $50d \times 5d \times 100d$ in x, y, z directions correspondingly. Periodic boundary conditions are applied in the y-direction. The orifice dimension is $10d \times 5d$.

Table 1. DEM material properties

Parameter	Value
Density (particle) ρ [kg/m^3]	4100
Coefficient of particle-particle friction μ^s_{pp}	0.56
Coefficient of particle-wall friction μ^s_{pw}	0.45
Coefficient of restitution (particles), e_p	0.15
Coefficient of restitution (wall), e_w	0.5
Poisson ratio (particles), ν_p	0.25
Poisson ratio (wall), ν_w	0.25
Shear modulus (particles), G_p[Pa]	10^7
Shear modulus (wall), G_w[Pa]	10^{10}

3 Results

3.1 Jenike Shear Test

Before comparing MS and SQ particles, simulations with mono-sized spherical particles were conducted to prove equivalence of the setups in the LIGGGHTS and EDEM codes. Results showed a reasonably good agreement with a maximum difference of 3 %.This discrepancy can be explained by the difference in initial particle configuration within the generated packings.

The DEM time-step was chosen as $\Delta t = 2 \cdot 10^{-6}$ s (5 % of Rayleigh time) in all simulations. Two types of packing, using MS and SQ particles, were generated to assess the dependency of the results on the density of the initial packing. In the dense packing, the particle-particle friction coefficient μ^s_{pp} was set to zero at the filling stage and changed back to $\mu^s_{pp} = 0.56$ before applying σ_v. On the contrary, the loose packing had $\mu^s_{pp} = 0.56$ during the whole simulation .

For all simulations, material properties were kept identical and packings were generated using SQ_{N4}, SQ_{N6}, SQ_{N8} and MS_8, MS_{27}, MS_{64} particles. Figure 3 presents the information on the volume of single MS and SQ particles (V_p) and the solid fraction (ϕ) of the packings for the shear tester. The results for ϕ are plotted against the ratio of V_p to the volume of the perfect cube ($V_c = 8$mm^3). It is observed that for MS particles, MS_8 has the lowest value of V_p/V_c, while the difference between MS_{27} and MS_{64} is much smaller. Additionally, the V_p/V_c value has a direct relation with N for SQ particles and $N = 8$ has the maximum value accordingly. For the solid fraction, it can be seen that MS_8 provides the packing with the largest ϕ. Furthermore, it is clear that for both loose and dense packings, SQ particles show an approximately constant value for ϕ (independent of the N value). MS_{27} and MS_{64} also follow the same trend for ϕ as SQ particles.

The corresponding shear stress curves for SQ and MS particles as a function of shear displacement (D) are repre-

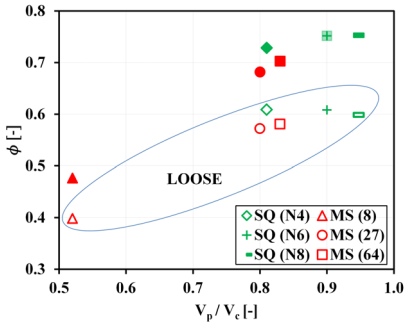

Figure 3. Solid fraction of the packings with different particle shapes (the filled markers are for dense packing)

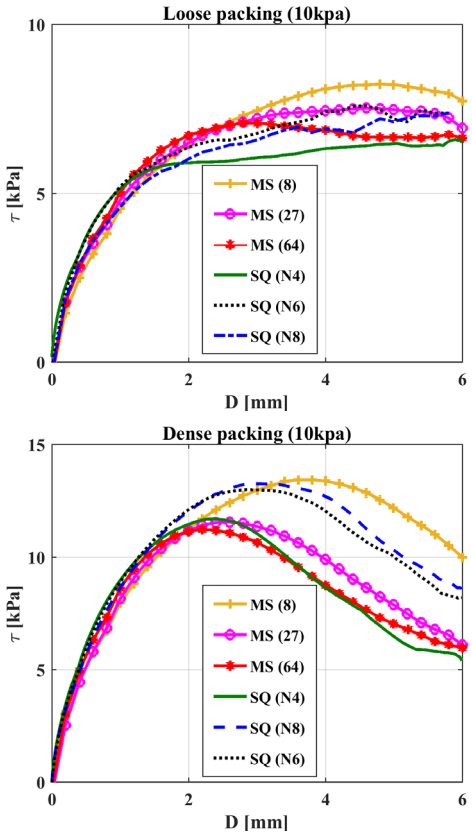

Figure 4. Jenike direct shear simulations considering SQ and MS particles a)loose packings b) dense packings.

sented in Fig. 4. It can be seen that, in loose packing, SQ_{N4} has the lowest strength during shearing. However, it can be noticed that after increasing the blockiness to $N = 6$, the material shows a higher strength, but a further blockiness (i.e. $N = 8$) plays no significant role in the shearing response of the SQ particles.

For the loose packings of the MS particles, the MS_{27} and MS_{64} show a similar peak strength, while a slightly lower residual strength can be seen for the MS_{64}. The MS_8 is providing a peak and residual strength larger than for MS_{27} and MS_{64}, which is an indication of increased interlocking among the MS_8 particles. Additionally, for the dense packing, increasing blockiness for SQ particles results in higher shear strength. A similar response is seen for the MS particles when the surface bumpiness is increased (i.e. the number of sub-spheres is reduced).

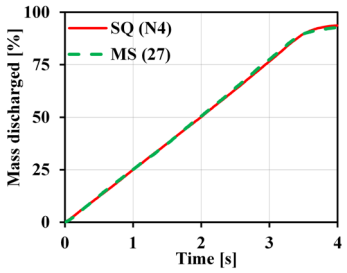

Figure 5. Cumulative discharged mass

It is also observed that SQ_{N4} is in good agreement with MS_{27} and MS_{64} and show a similar peak strength for the dense sample. Although in the loose samples the peak strength for SQ_{N4} stays approximately 15 % lower than MS_{27} and MS_{64}, the residual strength is relatively comparable. Accordingly, SQ_{N4} and MS_{27} and MS_{64} can be considered as numerically calibrated materials in a Jenike shear tester. The next section provides comparison of the macro-scale features of calibrated particles during silo flow. Due to the very high computational time for MS_{64}, the silo discharge is just simulated with MS_{27} particles and compared with results of SQ_{N4}.

3.2 Flat-bottom silo

Using the calibrated MS and SQ particles (MS_{27} and SQ_{N4}), a total of about 20 000 particles were generated in each software to model the filling and discharge of the flat-bottom silo. Figure 5 shows that the mass discharged is independent of the shape representation technique for the calibrated particles.

Snap-shots have been taken from different instances of the discharged mass (M_D) to provide an insight into flow profiles for both particle types. Figure 6 shows the particles inside the silo at 10, 30 and 60 % of the discharge. It can be seen that flow profiles are similar both in funnel and mass flow sections. This confirms the earlier results shown in Figure 5.

The wall pressure during discharge is also compared for both particle types. In this respect, the height of the wall is divided into equal-size bins and total normal contact forces are computed by using spatial averaging and plotted in Figure 7. Results are time-averaged over 0.05 seconds of the discharge to reduce the fluctuations of instantaneous values. Results show that there is significant difference between the two particles types at 10% of the discharge. This might be due to inappropriate spatial and temporal averaging windows or a result of the different initial particle configuration. However, it is clear that in the steady state stage of the discharge, the wall pressure distributions for the two particle types are in good agreement.

4 Conclusion

In this work, the behavior of SQ particles, at different edge sharpness levels, and MS particles, with different numbers of sub-spheres, have been evaluated in a Jenike shear test and the following conclusions are drawn:

• For the loose packings, the change in edge/corner sharpness (from $N = 4$ to $N = 6$) increases the strength o the

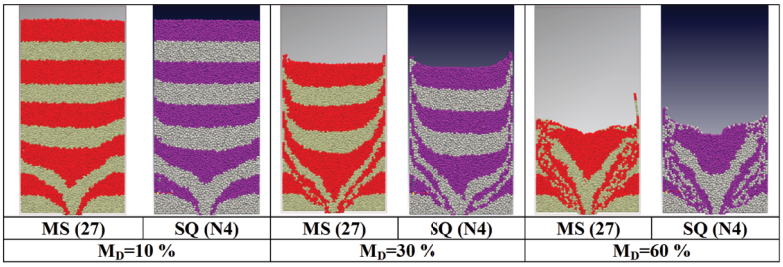

Figure 6. Flow profiles for both SQ and MS particles at M_D =10, 30 and 60 %

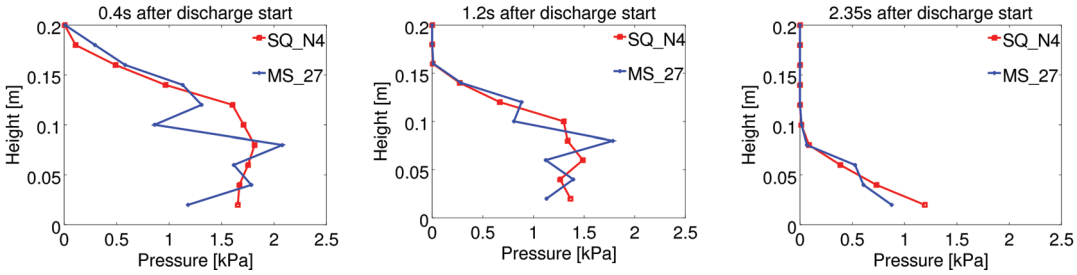

Figure 7. Normal wall pressure distribution along the height of the wall at 10%, 30% and 60% of the discharge (from left to right).

material. However, further increase of N plays no major role in the shearing response of SQ particles. For dense packing, increasing N leads to higher shearing resistance respectively for SQ particles.

• The bulk response of MS cubes is governed by the bumpiness of the surface in both loose and dense samples; the higher bumpiness, which means lower number of spheres contribute in building the surface of the single MS particle, increases the resistance of the material against shearing.

• It is also observed that the shearing result of SQ_{N4} is in good agreement with MS_{27} and MS_{64} and show a similar peak and residual strength in dense samples. For the loose samples, although the peak strength for SQ_{N4} is approximately 15 % lower than MS_{27} and MS_{64}, the residual strength is relatively comparable for these pair of particles (assumed as numerically calibrated particles).

The behaviour of the calibrated particles is also assessed during silo discharge and the key findings are:

• The discharge rate is matching well for MS_{27} and SQ_{N4} particles.

• Flow profiles are similar in both funnel and mass flow sections at various stages of the discharging process.

• The wall pressure distribution differs during the initial states of the discharge, however during steady state there is a good agreement between results for SQ and MS.

To sum up, by using a proper numerical calibration procedure (Jenike tester simulation), it is possible to select roughly equivalent SQ and MS representations that indeed produce very similar results in a silo flow simulation. However, further investigations are essential for generalization of the findings for various particle shapes.

Acknowledgments

This work has been carried out as a part of the T-MAPPP project, an EU-funded Framework 7 Marie Curie Initial Training Network. The financial support provided by the European Commission is gratefully acknowledged. The assistance received from Dr J. P. Morrissey is also acknowledged.

References

[1] J. Favier, M. Abbaspour-Fard, M. Kremmer, A. Raji, Engineering Computations **16**, 467 (1999)
[2] C. Kloss, C. Goniva, A. Hager, S. Amberger, S. Pirker, Progress in Computational Fluid Dynamics, An International Journal **12**, 140 (2012)
[3] P.W. Cleary, Engineering Computations **21**, 169 (2004)
[4] A. Podlozhnyuk, S. Pirker, C. Kloss, Computational Particle Mechanics (2016)
[5] P.W. Cleary, M.L. Sawley, Applied Mathematical Modelling **26**, 89 (2002)
[6] F.Y. Fraige, P.A. Langston, G.Z. Chen, Powder Technology **186**, 224 (2008)
[7] H. Tao, B. Jin, W. Zhong, X. Wang, B. Ren, Y. Zhang, R. Xiao, Chemical Engineering and Processing: Process Intensification **49**, 151 (2010)
[8] D. Markauskas, R. Kačianauskas, a. Džiugys, R. Navakas, Granular Matter **12**, 107 (2009)
[9] D. Solutions, Edinburgh, UK (2014)
[10] A.H. Barr, IEEE Computer Graphics and Applications **1**, 11 (1981)
[11] C. Zhou, J.Y. Ooi, Mechanics of Materials **41**, 707 (2009)
[12] J. Härtl, J.Y. Ooi, Powder Technology **212**, 231 (2011)